RSC Advances

PAPER

View Article Online
View Journal | View Issue

Cite this: *RSC Adv.*, 2019, **9**, 18050

Noninvasive diagnostic methods for diabetes mellitus from tear fluid†

Gabriela Glinská,[a] Kristína Krajčíková,[a] Katarína Zakutanská,[b] Oleg Shylenko,[c] Daria Kondrakhova,[c] Natália Tomašovičová,[b] Vladimír Komanický,[c] Jana Mašlanková[a] and Vladimíra Tomečková *[a]

Received 18th March 2019
Accepted 8th May 2019

DOI: 10.1039/c9ra02078k

rsc.li/rsc-advances

Diabetes mellitus and prolonged hyperglycemia can cause diabetic retinopathy. Diabetic retinopathy arises from damage to retinal vessels and, in its final stages, causes blindness. The early stages are often asymptomatic and although regular screening of diabetic patients is recommended, the beginning of diabetic retinopathy is insufficiently detected. The diagnostic potential of fluorescence spectroscopy, infrared spectroscopy and atomic force microscopy as the untraditional methods for diabetes mellitus was investigated using tear fluid. In our pilot study the structural changes of tear fluid of patients with diabetes mellitus after insulin and oral antidiabetic drug treatment was compared with healthy subjects. The results of analysis, infrared spectroscopy and atomic force microscopy confirmed structural changes in tear fluid of patients in comparison with the tear fluid of healthy subjects. Using new experimental laboratory methods in future could contribute to an improvement in diagnosis of diabetes mellitus and other selected ocular diseases using tear fluid.

1 Introduction

Tear fluid represents an alternative sampling material to "standard" biological fluids (blood and urine). Besides water, it consists of more than a thousand various proteins and peptides,[1] microRNAs,[2] vitamins,[3] hormones[4] and other compounds. The composition of tear fluid changes significantly during the presence of a disease,[5] which makes it, together with non-invasive collection, advantageous for diagnostics.

Diabetes mellitus is a metabolic disorder manifested by a high fasting blood glucose level (>7 mM) due to defects in insulin secretion or action. Prolonged hyperglycaemia caused protein glycation resulting in cardiomyopathy, nephropathy, neuropathy and retinopathy and can increase risk of glaucoma.[6] The major ocular symptoms of diabetes mellitus are haemorrhages, exudates and microaneurysms. Microaneurysms are focal dilatations of the retinal capillaries. They are the first malformation occurring in the eye during the disease. Diabetic retinopathy develops from damage to retinal vessels and, in its final stages, causes blindness. The early stages are often asymptomatic and although regular screening of diabetic patients is recommended, the beginning of diabetic retinopathy is insufficiently detected.

Diabetic retinopathy can be detected by visual acuity testing (measures the eye's ability to focus and to see details at near and far distances, and vision loss), ophthalmoscopy and slit lamp examination (which can detect the back of the eye and therefore changes in the retina), gonioscopy (find outs whether fluid drains out and causes blindness), tonometry (measures the intraocular pressure inside the eye) and optical coherence tomography (checks fluid in the retina). Sometimes a fluorescein angiogram is done. Assessment of diabetic retinopathy is done using fluorescein angiography to see what is happening in the retina. The dye travels through the blood vessels and a special camera takes a photo and shows if any blood vessels are blocked or leaking fluid or if any abnormal blood vessels are growing.[7]

Recently, numerous studies of the tear fluid of diabetic patients have started arising using mostly "omics" approaches.[8–11] Nguyen-Khuong *et al.* 2015 (ref. 8) compared tear glycosylation among patients with diabetes with and without retinopathy and healthy controls and found out that there were not significant changes as the disease developed and progressed. Stuard *et al.* 2017 (ref. 11) detected insulin-like growth factor binding protein-3 (IGFBP-3) in the basal tears of diabetic patients and control subjects, and found it was higher in diabetic patients and its levels correlated with the subbasal nerve plexus length and branch density indicating nerve fiber loss.[12] Costagliola *et al.* 2013 (ref. 13) observed the changes in TNF-α levels in the tear fluid of patients with proliferative and

[a]*Department of Medical and Clinical Biochemistry, Faculty of Medicine, Pavol Jozef Šafárik University in Košice, Trieda SNP 1, 040 11 Košice, Slovakia. E-mail: vladimira.tomeckova@upjs.sk*

[b]*Institute of Experimental Physics SAS, Watsonova 47, 040 01 Košice, Slovakia*

[c]*Department of Condensed Matter Physics, Institute of Physics, Faculty of Science, Pavol Jozef Šafárik University in Košice, Park Angelinum 9, 041 54 Košice, Slovakia*

† Electronic supplementary information (ESI) available. See DOI: 10.1039/c9ra02078k

non-proliferative diabetic retinopathy and healthy controls. TNF-α was increased in diabetic patients' tears and increased with the severity of pathology. Also, several other proteins have significantly dysregulated levels in tears, for example lipocalin,[10] endothelin-1,[14] lactotransferrin, lysozyme C and others.[15]

Methods for the determination of a particular substance in the sampling material provides the possibility of identification of a disease biomarker, an indicator of the presence and progress of a disease and response to a treatment. On the contrary, various spectroscopic methods also enable detection of the disease, however, without use of the specific biomarker. These methods include fluorescence spectroscopy (FS) which has been validated as a diagnostic tool during various pathologies, *e.g.* diastolic dysfunction,[16] non-small-cell lung carcinoma,[17] ischemic heart disease,[18] diabetes mellitus[19] and many others. The method is based on the analysis of the autofluorescent substances occurring in the sample (*e.g.* NAD^+, NADH, proteins, advanced glycation end products and others) the levels of which change during the pathology.

Next, the diagnostic potential of infrared spectroscopy (IRS) has been studied in atherosclerosis,[20] skin cancer,[21] multiple sclerosis[22] and others. It was also assessed as a monitoring tool for cerebral oxygenation.[23] Pathological conditions cause structural and functional changes in the biological system and, consequently, in the studied samples resulting in alterations in the vibrational spectra (although a molecule with a dipole moment is necessary) that are captured by infrared spectroscopy.

Another untraditional method is atomic force microscopy (AFM), which, although it does not belong to the spectroscopy group, could provide analysis of biological materials. In spite of the fact that it is mostly used for *in vitro* studies, such as for differentiating between normal and cancerous cells[24–26] or detection of viruses,[27] it is also used for novel studies and diagnostics. Examples of such studies include the detection of significant differences between the blood serum of patients and healthy controls, which were observed during ischemic heart disease[18] and breast cancer[28], together with assessment of changes in the dermis.[29]

In our pilot study we assessed the diagnostic potential of FS, IRS and AFM for diabetes mellitus using tear fluid.

2 Experimental

2.1 Materials

Physiological sodium chloride solution (0.9%) was purchased from B. Braun, Melsungen, Germany.

2.2 Tear samples

Tear fluid of healthy subjects ($n = 20$), of subjects with presbyopia ($n = 5$) and of patients with diabetes mellitus after insulin treatment ($n = 5$) and after oral antidiabetic drugs treatment ($n = 10$) was collected from an eye (from the left and right eyes separately) by a flushing method with saline solution. For example, the physiological salt solution ($V = 100$ μL) was added to the conjunctival sac of the left eye (the same procedure was repeated during the collection of tear fluid from the right eye). The flushed eye content was immediately collected by using a 100 μL micropipette in a plastic vacutainer microtube ($V = 200$ μL). The tear collection was realized by ophthalmologist MUDr. Gabriela Glinská in the Ophthalmology Clinic in Košice. After collection of tear fluids in vacutainer tubes, the tear samples were frozen and stored at a temperature of −80 °C until the measurements were carried out. All clinical investigations were conducted according to the declaration of Helsinki principles. Ethical consent for this study has been given by the institutional committee on human research and it is compliant with ethical standards on human experimentation and with the Helsinki declaration. The ethics committee per rollam gave a favorable opinion on tear collection from patients under protocol No. 7N/2015 and 7N/2018. From all the patients and healthy subjects informed consent was required.

2.3 Synchronous fluorescence fingerprint

For the synchronous fluorescence fingerprint, the intensity of fluorescence of each sample (tear fluid) was measured in a quartz cuvette (500 μL) after thawing by synchronous fluorescence fingerprint (SFF). The intensity of the total endogenous fluorescence of tear fluid as a complex was measured on a PerkinElmer Luminescence Spectrophotometer LS 55, $t = 25$ °C. The 10 simple synchronous spectra of tear fluid were measured at various $\Delta\lambda$ in the wavelength range $\lambda_{ex} = 200$–390 nm. The incremental distance between the simple spectra in space was $\Delta = 10$. The rate of the scans was 1200 nm s^{-1}. Both the excitation and emission slits were 5 nm. The resulting 3-D fluorescence synchronous fingerprint was processed using WinLab Software (version 4, 2001). The horizontal cut of SFF at $\Delta\lambda = 50$ revealed a simple synchronous spectrum with a peak of fluorescence. The synchronous fluorescence fingerprint measures the total fluorescence of all endogenous fluorophores in tear fluid. This rapid analysis of tear fluid as an unknown mixture provides more information in contrast to a simple synchronous spectrum.

2.4 Atomic force microscopy

An individual sample (10 μL) of tear fluid (healthy subjects and with diabetes mellitus) was deposited on the microscopic glass slides immediately after the synchronous fluorescence fingerprint had been measured and stretched over the surface by the method of blood smear. The slides were dried at room temperature without fixative. The samples were analyzed using the atomic force microscope Dimension Icon® (ICON, Bruker, Berkley, California, USA) in tapping mode with silicon tips (MikroMasch, Berkley, California, USA, NSC35 series) with a radius of curvature of 10 nm. The surface of each sample was processed by the software ScanAsyst™ software.

2.5 Infrared spectroscopy

The infrared spectra of the samples were measurements by the FTIR spectroscope Vertex 80-v (Bruker). 30 μL of sample was deposited on the ZnSe base and dried in a refrigerator for two

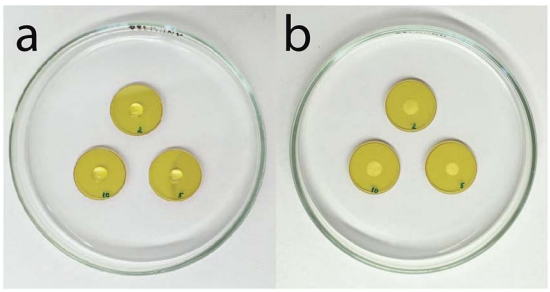

Fig. 1 Samples of tears (a) after deposition on ZnSe, (b) after drying.

days (Fig. 1). The dried samples were measured in transmission mode in air and under ambient temperature.

3 Results and discussion

3.1 Fluorescence spectroscopy

The intensity of fluorescence of tear fluids of patients with diabetes mellitus types I and II was studied and showed differences after different lengths of insulin and antidiabetic drug (OAD) treatment in comparison with the tear fluids of patients with diabetes mellitus without treatment and healthy subjects without diabetes mellitus. At first sight the synchronous fluorescence fingerprints of the tear fluid of patients with diabetes mellitus resembled those of control healthy subjects (Fig. 2, S1 and S2†) but detailed data analysis showed differences between the fluorescence of the tear fluid of diabetic patients (Fig. 2–4 and S1–S6†) and endogenous fluorescence of the tear fluid of control healthy subjects ($F = 721$, $\lambda = 278$ nm/$\Delta\lambda = 70$ nm).

Analysis of tear fluid of patients with untreated diabetes mellitus lasting 13 years (Fig. 2, S1 and S2†) showed lower endogenous fluorescence ($F = 531$) than intensity of fluorescence of tear fluid of healthy subjects ($F = 721$). The localization ($\lambda = 277$ nm/$\Delta\lambda = 70$ nm), structure and shape of the SFF were similar to those of healthy subjects ($\lambda = 278$ nm/$\Delta\lambda = 70$ nm) (see Table 1).

The synchronous fluorescence spectrum of tear fluid is specific for the control healthy subjects. It is considered to be a characteristic fingerprint. A simple comparison of spectra can confirm or disprove the identity of two samples of tear fluid during various diseases. This method enables the analysis of the multifluorescent mixture of tear fluid and its changes during diabetes mellitus. A detailed analysis of the fluorescence curve is not essential for the diagnosis. Changes of fluorophores under endogenous (elevated glucose) or exogenous stress factors (insulin and OAD treatment) in patients with diabetes mellitus disrupt the balance of mutual interactions of fluorophores in tear fluid. The result of diabetes mellitus is a modified graphical display due to the modified SFF. The result of diabetes mellitus is a modified SFF graphical display of tear fluid of healthy subjects and patients with diabetes mellitus show pathological changes as they show quantitative and qualitative information about changes of the tear fluid structure and characteristics for diagnostic assessment that could be used for the inexpensive, sensitive, accurate and rapid screening of diabetes mellitus. Fluorescence spectroscopy has not been used yet for research of tear fluid during various diabetes mellitus treatments but could be a new possibility in the early diagnosis of diabetes mellitus and other diseases.

3.1.1 OAD treatment. The lowest intensity of fluorescence ($F = 364$, $\lambda = 276$ nm/$\Delta\lambda = 70$ nm) was found for the tear fluid (Fig. 3, S3 and S4†) of patients with diabetes mellitus (with a presbyopia) after the first year of OAD treatment, compared to the tear fluid of healthy subjects ($F = 721$, $\lambda = 278$ nm/$\Delta\lambda = 70$ nm).

The tear fluid of patients with diabetes mellitus after 3 years OAD treatment with a presbyopia (Fig. 3, S3 and S4†) shows a similar intensity of fluorescence ($F = 724$), structure and shape of the SFF to the tear fluid of healthy subjects ($F = 721$), but the localization of the peak is different ($\lambda = 290$ nm/$\Delta\lambda = 60$ nm).

The tear fluid of patients after OAD treatment for 5 years with a presbyopia, glaucoma and cataract (Fig. 3, S3 and S4†) has a peak ($\lambda = 280$ nm/$\Delta\lambda = 60$ nm) with a lower fluorescence intensity ($F = 598$) in comparison to that of the tear fluid of control healthy subjects ($F = 721$, $\lambda = 278$ nm/$\Delta\lambda = 70$ nm).

The highest fluorescence ($F = 796$) was found from tear fluid of patients with diabetes mellitus after 7 years treatment with OAD at the fluorescence peak ($\lambda = 274$ nm/$\Delta\lambda = 70$ nm) of the 3-

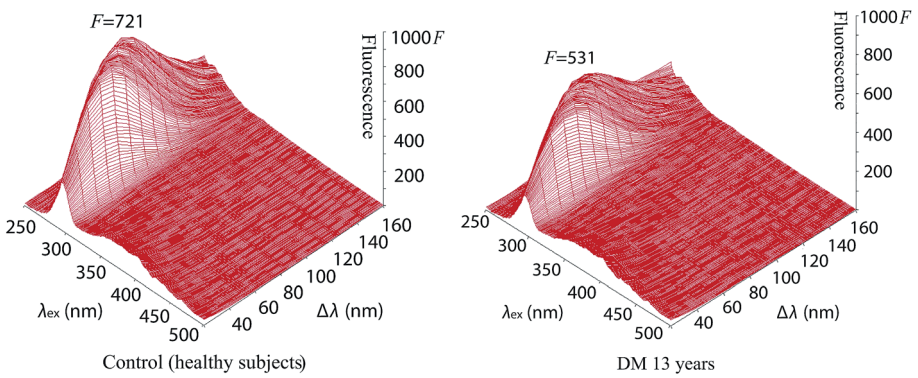

Fig. 2 Synchronous fluorescence fingerprint of tear fluid of patients without treatment of diabetes mellitus for 13 years in comparison with the synchronous fluorescence fingerprint of control (healthy subjects) tear fluid.

Table 1 Synchronous fluorescence fingerprint of tear fluid of patients with diabetes mellitus type 2 treated with OAD in comparison to the control sample and untreated diabetes mellitus

	Age	Wavelength (nm) $\lambda_{max}/\Delta\lambda$	F_{max}
Control sample	25	278/70	721
13 years untreated DM	50	277/70	531
DM 1 year on OAD	54	276/70	364
DM 3 years on OAD	55	290/60	724
DM 5 years on OAD	60	280/60	598
DM 7 years on OAD	42	274/70	796
DM 10 years on OAD	79	279/70	525

D and contour image of the synchronous fluorescence fingerprint (Fig. 3, S3 and S4†).

The tear fluid of the patients after OAD treatment for 10 years with a presbyopia, increased eye pressure, cataract and after myocardial infarction (Fig. 3, S3 and S4†) shows a peak ($\lambda = 279$ nm/$\Delta\lambda = 70$ nm) with a lower fluorescence intensity ($F = 525$) in comparison with that of the tear fluid of control healthy subjects ($F = 721$) but the localization of the peak was similar ($\lambda = 278$ nm/$\Delta\lambda = 70$ nm). The results for patients treated with OAD along with untreated diabetes mellitus are summarized in Table 1.

The center of the endogenous fluorescence of the tear fluid of patients with diabetes mellitus (in combination with presbyopia) treated with oral antidiabetic drugs for 1 year showed the lowest fluorescence ($\lambda_{ex} = 284$ nm, $F = 325$) in comparison with that of the tear fluid of patients with diabetes mellitus treated with oral antidiabetic drugs for 5 years ($\lambda_{ex} = 284$ nm, $F = 554$) and 10 years ($\lambda_{ex} = 282$ nm, $F = 473$). The endogenous fluorescence of the tear fluid of healthy subjects ($\lambda_{ex} = 289$ nm, $F = 721$) was similar to that of the tear fluid of patients with diabetes mellitus treated with oral antidiabetic drugs for 3 years ($\lambda_{ex} = 292$ nm, $F = 722$) but the shape of the spectrum was similar to that of the tear fluid of patients with diabetes mellitus treated with oral antidiabetic drugs for 7 years, which showed the highest fluorescence ($\lambda_{ex} = 289$ nm, $F = 796$).

Comparison of the endogenous fluorescence at $\lambda_{ex} = 280$ nm and $\Delta\lambda = 50$ nm showed that the highest fluorescence was for the tear fluid of patients with diabetes mellitus treated with oral antidiabetic drugs for 7 years ($F = 678$) in comparison with the tear fluid of healthy subjects ($F = 655$) and the tear fluid of patients with diabetes mellitus treated with oral antidiabetic drugs for 3 years ($F = 606$). The lowest intensity of fluorescence was found for the tear fluid of patients with diabetes mellitus treated with oral antidiabetic drugs for 1 year ($F = 320$). A low intensity of fluorescence was found for the tear fluid of patients with diabetes mellitus treated with oral antidiabetic drugs for 5 years ($F = 535$). A slightly lower intensity of fluorescence was found for the tear fluid of patients with diabetes mellitus treated with oral antidiabetic

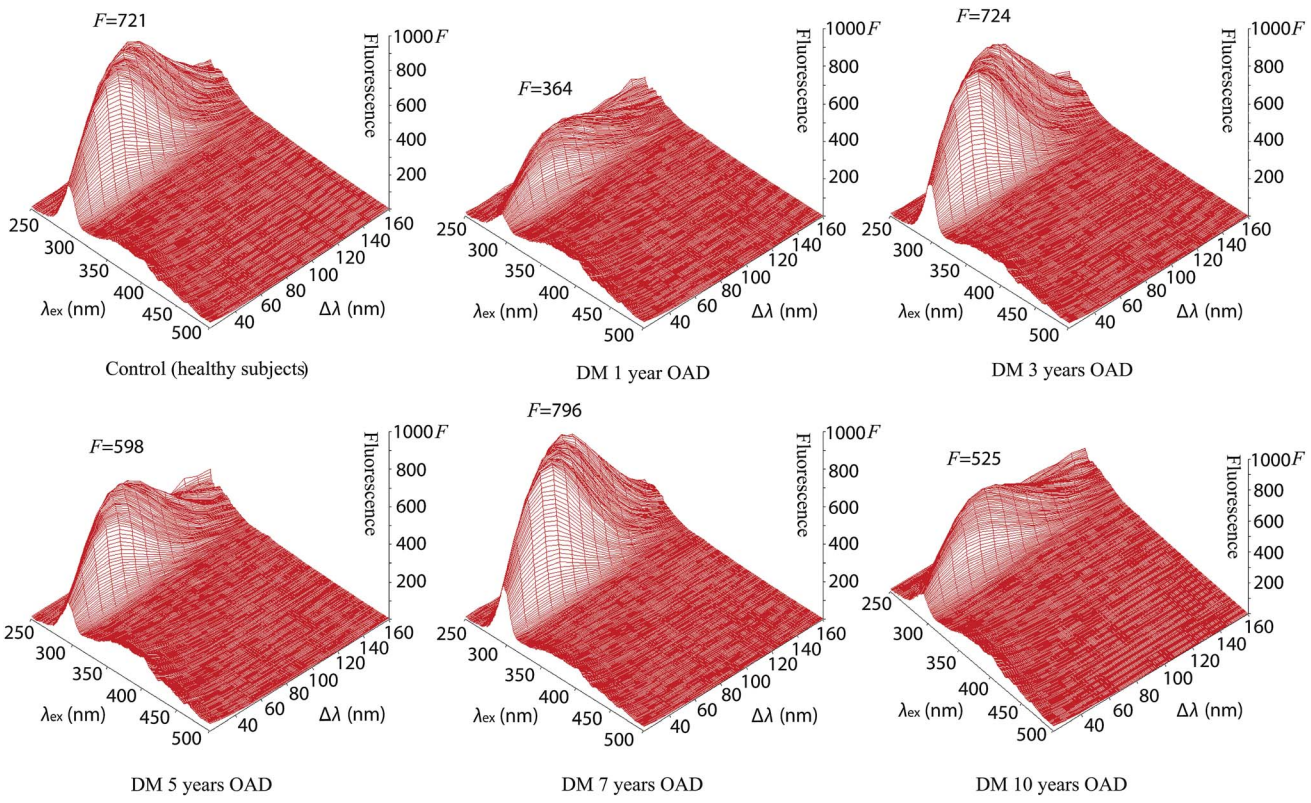

Fig. 3 Comparison of synchronous fluorescence fingerprints of tear fluid after antidiabetic drug treatment with various treatment lengths and that of the tear fluid of the control (healthy subjects).

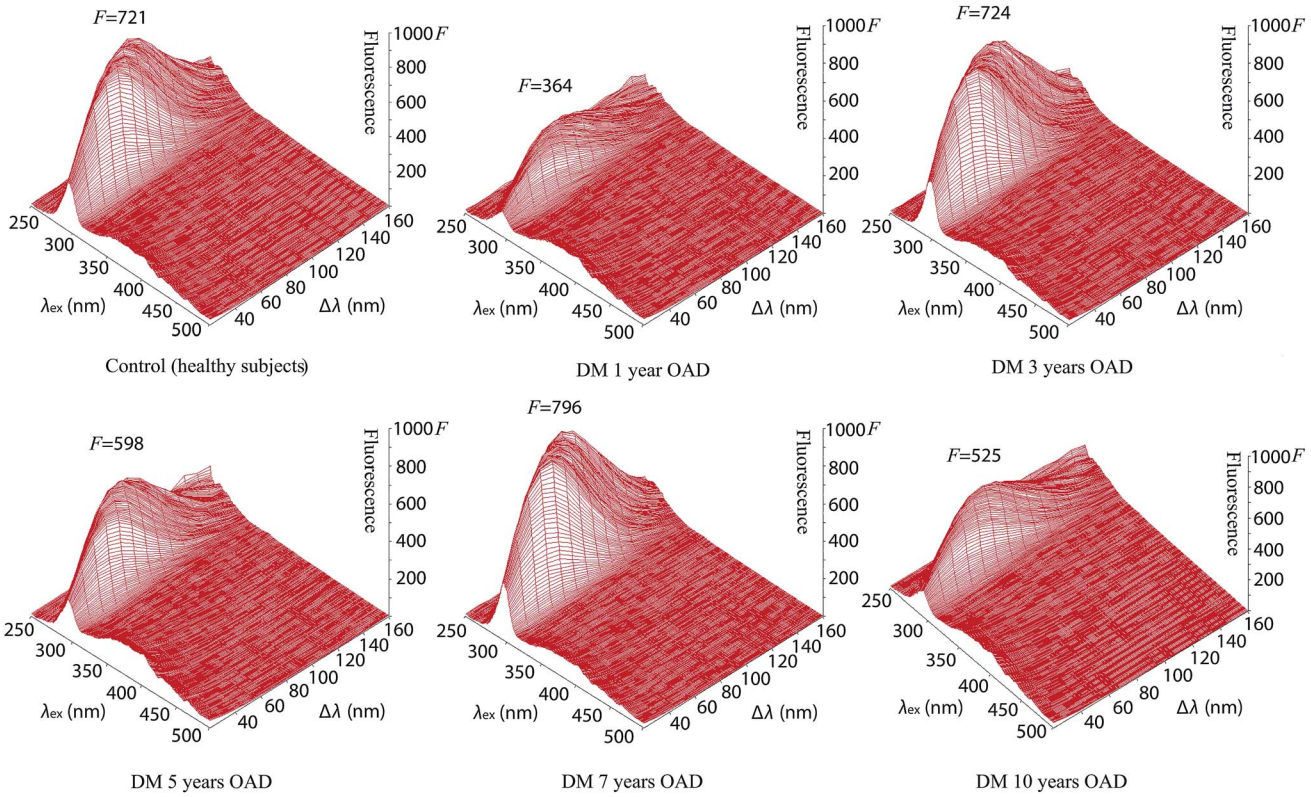

Fig. 4 Synchronous fluorescence fingerprints of the tear fluid of patients with diabetes mellitus type 1 and type 2 treated with insulin in comparison to the control sample.

Table 2 Fluorescence peaks of the tear fluid of patients with diabetes mellitus treated with OAD and insulin in comparison to the control sample and untreated diabetes mellitus

	Age	Wavelength (nm) $\lambda_{max}/\Delta\lambda$	F_{max}
Control sample	25	278/70	721
DM 14 years on insulin	47	277/70	626
DM 20 years on insulin	71	279/60	771
DM 25 years on insulin	49	279/70	409

drugs for 10 years ($F = 465$) in comparison with intensity of fluorescence of the tear fluid of untreated diabetes mellitus patients ($F = 470$).

3.1.2 Insulin treatment. Tear fluid of the patients with diabetes mellitus type 2 treated with insulin for 14 years (Fig. 2, S1, S2, 4, S5 and S6†) showed a peak ($\lambda = 277$ nm/$\Delta\lambda = 70$ nm) with a lower fluorescence intensity ($F = 626$) than that of tear fluid of control healthy subjects, but the location of the peak was similar ($F = 721$, $\lambda = 278$ nm/$\Delta\lambda = 70$ nm). The tear fluid of a patient with type 2 diabetes mellitus after 20 years of insulin treatment displayed a peak ($\lambda = 279$ nm/$\Delta\lambda = 60$ nm, $F = 771$) with a different SFF structure and shape (Fig. 2, S1, S2, 4, S5 and S6†). This patient had an artificial intraocular lens implanted after retinal laser therapy. Diabetes mellitus is a systematic disease that can cause other associated ocular complications,

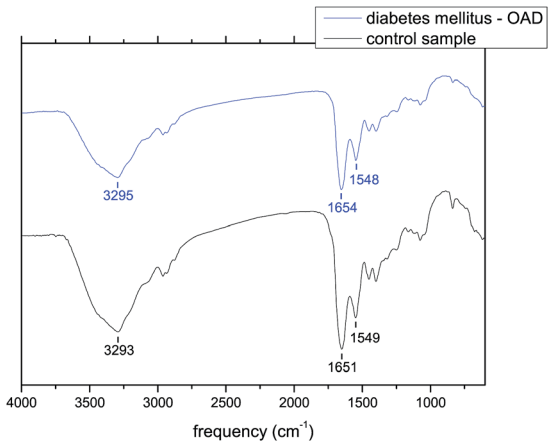

Fig. 5 Diabetes mellitus on OAD (7 years) in comparison to the control sample. Peaks around 3300 cm^{-1} are mainly caused by N–H stretching vibrations, peaks around 1650 cm^{-1} are mostly caused by C=O stretching vibrations and peaks around 1550 cm^{-1} are caused by in-plane bending vibrations, N–H stretching vibrations and C–C stretching vibrations.

for example diabetes retinopathy, cataracts, glaucoma and dry eye disease. All patients had confirmed diabetes mellitus and presbyopia. The lowest intensity of fluorescence ($F = 409$, $\lambda = 279$ nm/$\Delta\lambda = 70$ nm) was found for the tear fluid of the patients with inherited type 1 diabetes mellitus after 25 years of

Table 3 Diabetes mellitus on OAD samples in comparison to the control sample

	Age	Amide A (cm^{-1})	Amide I (cm^{-1})	Amide II (cm^{-1})
Control sample	25	3293	1651	1549
DM 1 year on OAD	54	3317	1657	1547
DM 3 years on OAD	55	3293	1649	1551
DM 5 years on OAD	60	3285	1650	1543
DM 7 years on OAD	42	3295	1654	1548
DM 10 years on OAD	79	3317	1647	1543

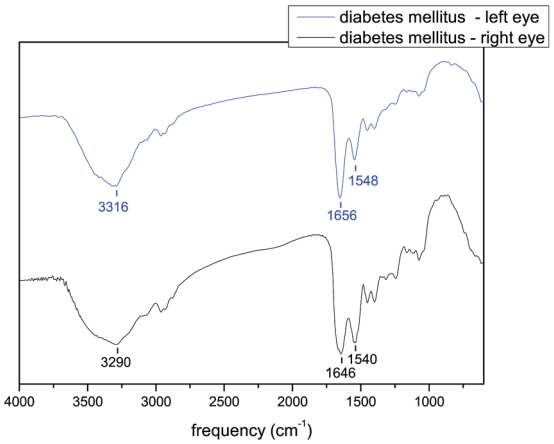

Fig. 6 Diabetes mellitus untreated for 13 years, in the presence of OAD – comparison of the left and right eye. Peaks around 3300 cm^{-1} are mainly caused by N–H stretching vibrations, peaks around 1650 cm^{-1} are mostly caused by C=O stretching vibrations and peaks around 1550 cm^{-1} are caused by in-plane bending vibrations, N–H stretching vibrations and C–C stretching vibrations.

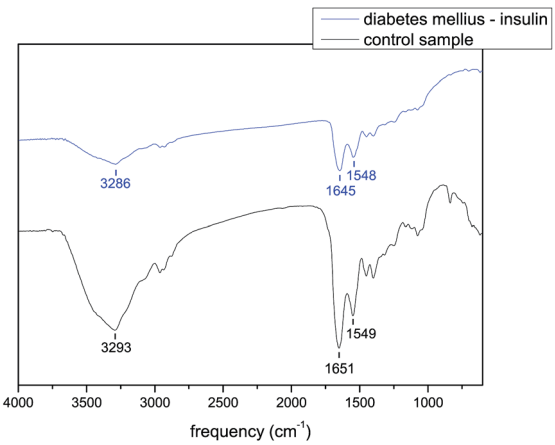

Fig. 7 Diabetes mellitus on insulin (25 years) sample in comparison to the control sample. Peaks around 3300 cm^{-1} are mainly caused by N–H stretching vibrations, peaks around 1650 cm^{-1} are mostly caused by C=O stretching vibrations and peaks around 1550 cm^{-1} are caused by in-plane bending vibrations, N–H stretching vibrations and C–C stretching vibrations.

insulin treatment with a confirmed dry eye (Fig. 2, S1, S2, 4, S5 and S6†). The results for patients treated with insulin are summarized in Table 2.

The endogenous fluorescence of the tear fluid of healthy subjects (λ_{ex} = 289 nm, F = 721) was higher than that of the tear fluid of patients with diabetes mellitus treated with insulin for 14 years (λ_{ex} = 285 nm, F = 555). The endogenous fluorescence of the tear fluid of patients with untreated diabetes mellitus for 13 years was λ_{ex} = 288 nm, F = 497. The tear fluid of patients with diabetes mellitus treated with insulin (in combination with dry eye) for 25 years (λ_{ex} = 283 nm, F = 371) showed a similar peak position to that of the tear fluid of patients with diabetes mellitus treated with insulin for 20 years (λ_{ex} = 283 nm, F = 722), but it exhibited a similar endogenous fluorescence to that for healthy subjects.

Comparison of endogenous fluorescence at λ_{ex} = 280 nm and $\Delta\lambda$ = 50 nm showed that the highest fluorescence was for the tear fluid of patients with diabetes mellitus treated with insulin for 20 years (F = 700) in comparison with that of the tear fluid of healthy subjects (F = 655) and the tear fluid of patients with diabetes mellitus treated with insulin for 14 years (F = 538). The lowest intensity of fluorescence was shown for the tear fluid of patients with inherited diabetes mellitus treated with insulin (in combination with dry eye) for 25 years (F = 354).

3.2 Infrared spectroscopy

One of the methods used for studying the effect of varied physiological factors on protein structure is infrared spectroscopy. There are 9 characteristic peaks in the infrared spectra of proteins – amide A, B and I–VII. Amide A is located at around 3300 cm^{-1} and it is mainly caused by N–H stretching vibrations (more than 95%). Amide B is located at around 3100 cm^{-1} and the cause of this peak is also N–H stretching vibrations. The most significant peaks in the infrared spectra of proteins are amide I and amide II. Amide I, with a position of 1600–1700 cm^{-1}, is caused by C=O stretching vibrations (70–85%) and amide II, with a position of 1510–1580 cm^{-1}, is caused by in-plane C–N bending vibrations (40–60%), N–H stretching vibrations (18–40%) and C–C stretching vibrations (approximately 10%). Amide III (1229–1301 cm^{-1}), amide IV (625–767 cm^{-1}), amide V (640–800 cm^{-1}), amide VI (537–606 cm^{-1}) and amide VII (approximately 200 cm^{-1}) are very complex, and therefore they are not suitable for studying proteins.[30]

In the case of diabetes mellitus treated with an OAD the position of amide A differs from 3293 to 3317 cm^{-1}, amide I is located in the range of 1647–1657 cm^{-1} and the positions of amide II are in the range of 1543–1551 cm^{-1}. In the case of diabetes mellitus treated with insulin the position of amide A is located around 3286 cm^{-1}, the position of amide I differs from 1645 to 1652 cm^{-1}

Table 4 Diabetes mellitus untreated for 13 years, in the presence of OAD – comparison of left and right eyes

	Age	Amide A (cm^{-1})	Amide I (cm^{-1})	Amide II (cm^{-1})
Control sample	25	3293	1651	1549
DM – left eye	50	3316	1656	1548
DM – right eye	50	3290	1646	1540

Table 5 Diabetes mellitus on insulin in comparison to the control sample

	Age	Amide A (cm^{-1})	Amide I (cm^{-1})	Amide II (cm^{-1})
Control sample	25	3293	1651	1549
DM 14 years on insulin	47	3286	1652	1540
DM 20 years on insulin	71	3285	1648	1542
DM 25 years on insulin	49	3286	1645	1548

and the frequencies of amide II are in the range of 1540–1548 cm^{-1}. For comparison, the position of amide A is 3293 cm^{-1}, the position of amide I is 1651 cm^{-1} and the position of amide II is 1549 cm^{-1} for the control sample. The infrared spectra of the tear samples of the patients with diabetes mellitus on oral antidiabetic drugs and the infrared spectra of the tear samples of the patients with diabetes mellitus on insulin are summarized in Fig. 5–7 and in Tables 3–5. As it is seen from these figures and tables the spectra of tears of patients with diabetes mellitus differ from those of the control sample as well as between each other. Fig. 5 shows the spectrum of the diabetes mellitus with 7 years on OAD sample in comparison to that of the control sample and Fig. 7 shows the spectrum of the diabetes mellitus with 25 years on insulin sample in comparison to that of the control sample.

Similarly, when the infrared spectra of the left and right eye tear samples of a patient with untreated diabetes mellitus 13 years on OAD are compared, it is possible to see differences in amide A, amide I and amide II positions. Peak position is most different in the case of amide A. The frequency of amide A is 3316 cm^{-1} for the left eye and 3290 cm^{-1} for the right eye. For the control sample the peak position is 3293 cm^{-1}. Amide I is located at 1656 cm^{-1} for the left eye and 1646 cm^{-1} for the right

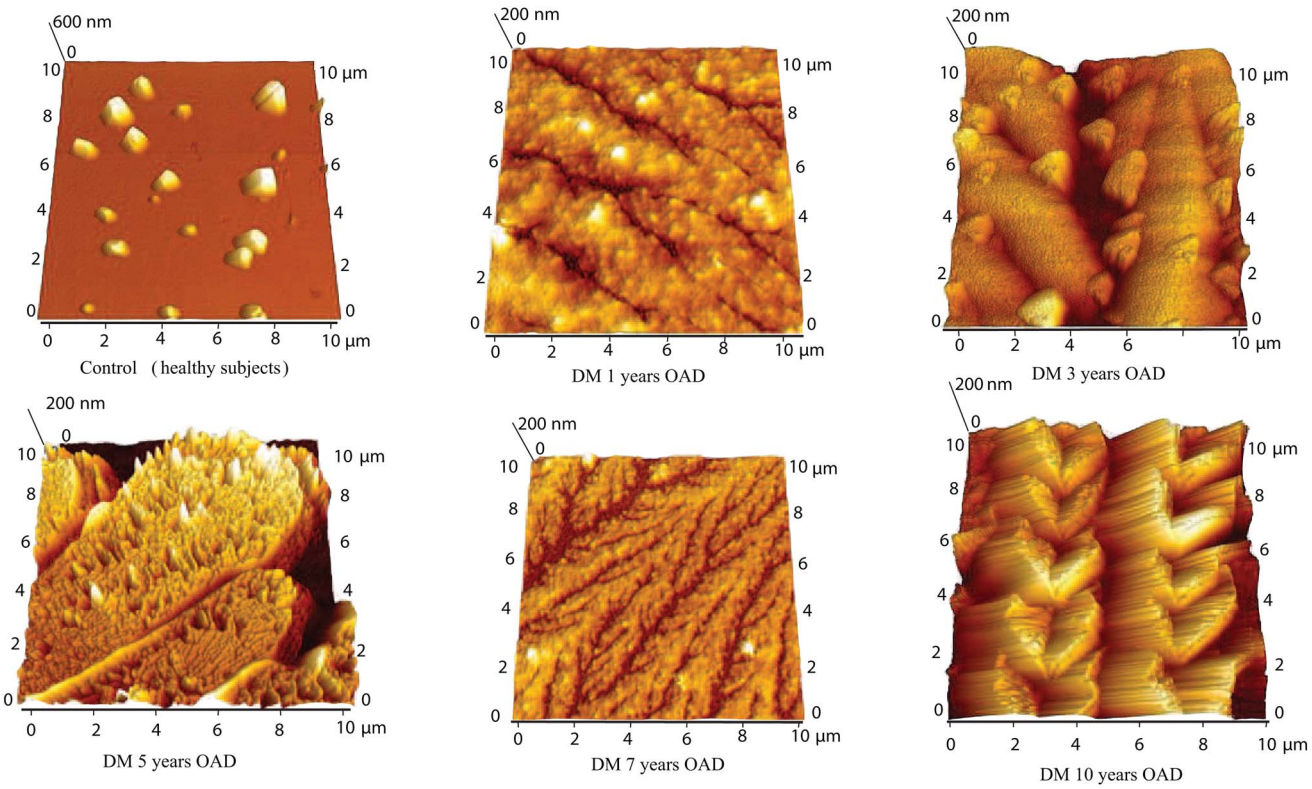

Fig. 8 Comparison of atomic force microscopy of control (healthy subjects) tear fluid and the tear fluid of patients after antidiabetic drug treatment with various treatment lengths.

eye. Both of these values are different from the value of 1651 cm^{-1} that is the location of amide A in the case of the control sample. Additionally, the positions of amide II in the case of the left and right eyes differ from each other as well. The position of the peak for the right eye is 1540 cm^{-1} and the position of the peak for the left eye is 1548 cm^{-1}, which is close to the peak position of the control sample of 1549 cm^{-1}. The peak positions are listed in the Table 4. Fig. 6 shows the infrared spectra of the left and right eye tear samples.

The differences in the infrared spectra may be caused by various factors. Besides the effect of the disease on the infrared spectra of proteins, the spectra are affected also by vision quality, eye pressure, genetic factors, time of collection, ocular dominance *etc.*[31] The differences in the spectra confirms the differences in protein structure, that are affected by health condition.

3.3 Atomic force microscopy

The various characteristic structures were observed in the tear fluid of patients with diabetes mellitus by atomic force microscopy. Separated crystals of 300–1000 nm and a surface roughness of 81 nm were observed in the tear fluid of healthy subjects (Fig. 8 and 9). The simple comparing of the tear fluid of patients with diabetes mellitus can show characteristic changes of the tear structures based on the duration of the disease, the type of selected treatment with antidiabetic drug treatment (Fig. 8) or insulin treatment (Fig. 9). A dense network of dendrites has been observed on the surface of samples from patients with diabetes mellitus with 1 year on OAD in combination with presbyopia. The main branch had a length of 30–40 μm and the lateral branches were 8–10 μm. The dendrites had small fine grains of 50–100 nm. The total surface roughness was 19 nm. Dendrites with major branches of more than 50 μm long and 1.3 μm wide and other secondary fibers with a thickness of 1.2 μm have been observed on the surface of samples from patients with diabetes mellitus on OAD for 3 years. These fibers were coated with 0.5 μm small crystals. The surface roughness was 79.6 nm.

A large dendritic plaque has been observed on the surface of samples from patients with diabetes mellitus after 5 years on OAD. The main branches had a thickness of 5–9 μm and a length of more than 50 μm. The lateral branches were 7–14 μm long and 5–9 μm wide, and small branches 7–14 μm long have a thickness of 2–7 μm. The roughness of the surface was 115 mm. Fine dendrites with a high degree of branching with lengths 6–22 μm were observed on the surface of the samples with diabetes mellitus after 7 years on OAD. The branches had approximately the same thickness of 300–400 nm and the total roughness of the surface was 14.7 nm. At the surface of the tear fluid of patients with diabetes mellitus after 10 years on OAD heart-shaped crystals connected in chains of 17–20 μm length and with 3.5 μm width were observed. The individual crystals were probably formed due to the crystallization of glucose and salts with proteins. The total surface roughness was 89 nm. The overall morphology in the AFM images was very different for patients

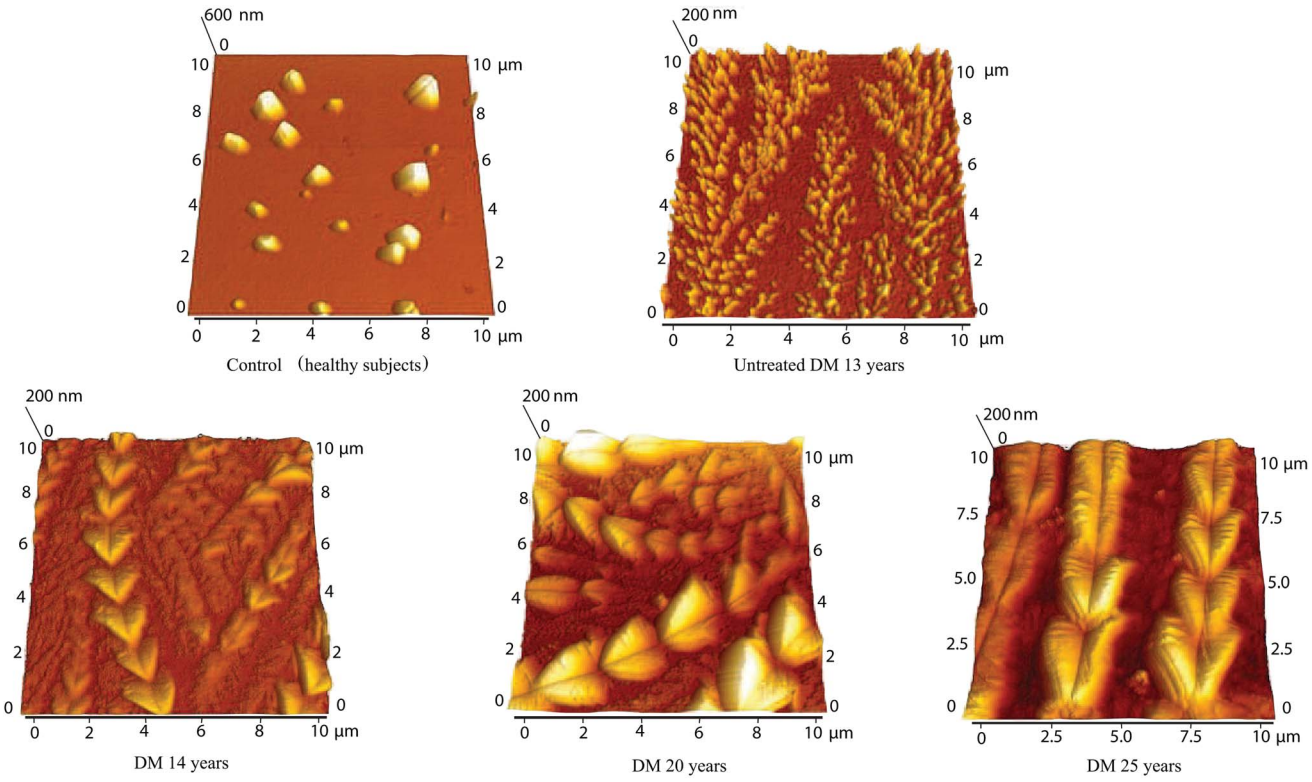

Fig. 9 Comparison of atomic force microscopy of control (healthy subjects) tear fluid and the tear fluid of patients after insulin treatment with various treatment lengths.

treated with OAD. No similarities were observed which indicates that different compounds were responsible for creating the crystalline dendrites observed by AFM. This is in agreement with IR data where no correlation in peak position was observed for this chosen group of patients. The morphology of the samples made from the tears of patients with untreated diabetes mellitus for 13 years (Fig. 9) shows dendrites fragmented into tiny grains (100–300 nm with roughness 24.4 nm). Several formations resembling wheat ear-shaped crystals of 15–30 nm in length composed of the hearts with size 0.5–1.5 μm (some growing centrally from one point) were observed on the surface of the tear fluid of patients with diabetes mellitus after 14 years treatment with insulin. The total surface roughness was 20 nm. Isosceles triangles with a shoulder length of 2 μm were observed on the surface of the tear fluid of patients with diabetes mellitus after 20 years treatment with insulin. The strands were 10 μm long and the surface roughness was 33.3 nm. The surface of the tear fluid of the patient with diabetes mellitus in combination with dry eye after 25 years treatment with insulin contains chains composed of hearts with lengths up to 50 μm. The size of the heart was 0.8–3 μm. Branches with length 2–10 μm and width 0.5 μm were present in the background. The surface roughness was 43.3 nm. It can be concluded that all patients treated with insulin have similar structures. This is in agreement with IR data where similarities in amide A peak positions are observed for this group of patients.

It is known that proteins form dendritic structures depending on various factors during evaporation. For example, the effect of pH on the formation and shape of protein nanostructures was studied in the work of Dogra *et al.* 2017.[32] Formation of protein structures during evaporation of a solution containing two types of protein was studied by Carreón *et al.* 2018.[33] Furthermore, Rojas *et al.* 2017 studied the effect of the neurotransmitter serotonin on dendritic structure.[34]

4 Conclusions

Tear fluid sensitively reveals changes in the body and thus becomes the object of an appropriate sensitive examination by using untraditional novel techniques: synchronous fluorescence fingerprint, atomic force microscopy and infrared spectroscopy. These methods showed mutual supporting and confirming results which can quickly identify changes in the structure of tear fluid, *e.g.* different crystallization and conversion of the globular ordered structure of proteins to a fibrillar disordered structure (dendrites and heart shape structure), in the presence of diabetes mellitus. The significant differences in the structure of tear fluid of healthy subjects in comparison with tear fluid of patients with untreated diabetes mellitus and diabetes mellitus treated with oral antidiabetic drugs and insulin were observed. The presented results suggest the close relation of the crystal structure of tear fluid in the presence of treated and untreated diabetes mellitus suggesting the possible use of tear fluid detection as a non-invasive diagnosis tool during diabetes mellitus pathologies.

Conflicts of interest

The authors state that there is no financial relationship to disclose and have no conflict of interest to declare.

Acknowledgements

This study was carried out with the support of the following grants: VVGS 2018-747, VEGA 2/0016/17 and the ERDF EU grant under the contracts No. ITMS26220120047. This work has been supported by grant VEGA No. 1/0204/18.

Notes and references

1 J. H. Jung, Y. W. Ji, H. S. Hwang, J. W. Oh, H. C. Kim, H. K. Lee and K. P. Kim, *Sci. Rep.*, 2017, **7**, 13363.
2 J. A. Weber, D. H. Baxter, S. Zhang, D. Y. Huang, K. H. Huang, M. J. Lee, D. J. Galas and K. Wang, *Clin. Chem.*, 2010, **56**, 1733–1741.
3 X. Lu, R. A. Elizondo, R. Nielsen, E. I. Christensen, J. Yang, B. D. Hammock and M. A. Watsky, *Invest. Ophthalmol. Visual Sci.*, 2015, **56**, 5880–5887.
4 D. Pieragostino, L. Agnifili, I. Cicalini, R. Calienno, M. Zucchelli, L. Mastropasqua, P. Sacchetta, P. Del Boccio and C. Rossi, *Int. J. Mol. Sci.*, 2017, **18**, 1349.
5 S. Hagan, E. Martin and A. Enríquez-de Salamanca, *EPMA J.*, 2016, **7**, 15.
6 V. P. Singh, A. Bali, N. Singh and A. S. Jaggi, *Korean J. Physiol. Pharmacol.*, 2014, **18**, 1–14.
7 G. Mahendran and R. Dhanasekaran, *Comput. Electr. Eng.*, 2015, **45**, 312–323.
8 T. Nguyen-Khuong, A. V. Everest-Dass, L. Kautto, Z. Zhao, M. D. P. Willcox and N. H. Packer, *Glycobiology*, 2015, **25**, 269–283.
9 Z. Torok, T. Peto, E. Csosz, E. Tukacs, A. M. Molnar, A. Berta, J. Tozser, A. Hajdu, V. Nagy, B. Domokos and A. Csutak, *J. Diabetes Res.*, 2015, **2015**, 623619.
10 J.-C. Wang, H.-Y. Ku, T.-S. Chen and H.-S. Chuang, *Biosens. Bioelectron.*, 2017, **89**, 701–709.
11 W. L. Stuard, R. Titone and D. M. Robertson, *Invest. Ophthalmol. Visual Sci.*, 2017, **58**, 6105–6112.
12 N. Papanas and D. Ziegler, *J. Diabetes Invest.*, 2015, **6**, 381–389.
13 C. Costagliola, V. Romano, M. De Tollis, F. Aceto, R. dell′Omo, M. R. Romano, C. Pedicino and F. Semeraro, *Mediators Inflammation*, 2013, **2013**, 629529.
14 T. A. Pavlenko, N. B. Chesnokova, H. G. Davydova, T. D. Okhotsimskaia, O. V. Beznos and A. V. Grigor'ev, *Vestn. Oftalmol.*, 2013, **129**, 20–23.
15 E. Csősz, P. Boross, A. Csutak, A. Berta, F. Tóth, S. Póliska, Z. Török and T. József, *J. Proteomics*, 2012, **75**, 2196–2204.
16 C.-C. Wang, Y.-C. Wang, G.-J. Wang, M.-Y. Shen, Y.-L. Chang, S.-Y. Liou, H.-C. Chen, A.-S. Lee, K.-C. Chang, W.-Y. Chen and C.-T. Chang, *Cardiovasc. Diabetol.*, 2017, **16**, 15.
17 H. Takizawa, K. Kondo, N. Kawakita, M. Tsuboi, H. Toba, K. Kajiura, Y. Kawakami, S. Sakiyama, A. Tangoku,

A. Morishita, Y. Nakagawa and T. Hirose, *Eur. J. Cardiothorac. Surg.*, 2018, **53**, 987–992.

18 V. Tomečková, V. Komanický, M. Kakoush, K. Krajčíková, G. Glinská, M. Široká, L. Pundová, T. Samuely, D. Hložná and D. Lotnyk, *Spectral Anal. Rev.*, 2016, **4**, 11–22.

19 B. T. Fokkens, R. van Waateringe, D. Mulder, B. H. Wolffenbutel and A. J. Smit, *Diabetes Metab.*, 2017, **44**, 424–430.

20 A. S. Peters, J. Backhaus, A. Pfüetzner, M. Raster, G. Burgard, S. Demirel, D. Böckler and M. Hakimi, *Vib. Spectrosc.*, 2017, **92**, 20–26.

21 E. Hägerlind, M. Falk, T. Löfstedt, B. Lindholm-Sethson and I. Bodén, *Skin Res. Technol.*, 2015, **21**, 493–499.

22 D. Yonar, L. Ocek, B. I. Tiftikcioglu, Y. Zorlu and F. Severcan, *Sci. Rep.*, 2018, **8**, 1025.

23 C. Rummel, R. Basciani, A. Nirkko, G. Schroth, M. Stucki, D. Reineke, B. Eberle and H. A. Kaiser, *J. Biomed. Opt.*, 2018, **23**, 016012.

24 M. Lekka, D. Gil, K. Pogoda, J. Dulińska-Litewka, R. Jach, J. Gostek, O. Klymenko, S. Prauzner-Bechcicki, Z. Stachura, J. Wiltowska-Zuber, K. Okon and P. Laidler, *Arch. Biochem. Biophys.*, 2012, **518**, 151–156.

25 E. Canetta, A. Riches, E. Borger, S. Herrington, K. Dholakia and A. K. Adya, *Acta Biomater.*, 2014, **10**, 2043–2055.

26 J. R. Staunton, B. L. Doss, S. Lindsay and R. Ros, *Sci. Rep.*, 2016, **6**, 19686.

27 Y. D. Ivanov, A. L. Kaysheva, P. A. Frantsuzov, T. O. Pleshakova, N. V. Krohin, A. A. Izotov, I. D. Shumov, V. F. Uchaikin, V. A. Konev, V. S. Ziborov and A. I. Archakov, *Int. J. Nanomed.*, 2015, **10**, 1597–1608.

28 I. Špaková, M. Ferenčáková, M. Rabajdová, V. Tomečková, V. Komanický and M. Mareková, *Curr. Metabolomics*, 2018, **6**, 2–9.

29 L. Peñuela, C. Negro, M. Massa, E. Repaci, E. Cozzani, A. Parodi, S. Scaglione, R. Quarto and R. Raiteri, *Exp. Dermatol.*, 2018, **27**, 150–155.

30 A. Jabs, *Determination of Secondary Structure in Proteins by Fourier Transform Infrared Spectroscopy (FTIR)*, Jena Library of Biological Macromolecules, 2015.

31 Y. Nagase, S. Yoshida and K. Kamiyama, *Biopolymers*, 2005, **79**, 18–27.

32 P. Dogra, M. Bhattacharya and S. Mukhopadhyay, *J. Phys. Chem. B*, 2017, **121**, 412–419.

33 Y. J. P. Carreón, J. González-Gutiérrez, M. I. Pérez-Camacho and H. Mercado-Uribe, *Colloids Surf., B*, 2018, **161**, 103–110.

34 P. S. Rojas, F. Aguayo, D. Neira, M. Tejos, E. Aliaga, J. P. Muñoz, C. S. Parra and J. L. Fiedler, *Mol. Cell. Neurosci.*, 2017, **85**, 148–161.